[CANCER RESEARCH 61, 6185–6193, August 15, 2001]

Loss of p53 Function Confers High-Level Multidrug Resistance in Neuroblastoma Cell Lines[1]

Nino Keshelava, Juan J. Zuo, Ping Chen, Sitara N. Waidyaratne, Marian C. Luna, Charles J. Gomer, Timothy J. Triche, and C. Patrick Reynolds[2]

Division of Hematology-Oncology, Children's Hospital Los Angeles, Los Angeles, California 90027 [N. K., J. J. Z., P. C., S. N. W., M. C. L., C. J. G., T. J. T., C. P. R.], and Departments of Pediatrics [N. K., J. J. Z., P. C., M. C. L., C. J. G., C. P. R.] and Pathology [S. N. W., T. J. T.], University of Southern California School of Medicine, Los Angeles, California 90033

ABSTRACT

Neuroblastomas can acquire a sustained high-level drug resistance during chemotherapy and especially myeloablative chemoradiotherapy. p53 mutations are rare in primary neuroblastomas, but a loss of p53 function could play a role in multidrug resistance. We determined p53 function by measuring induction of p21 and/or MDM2 proteins in response to melphalan (L-PAM) in seven L-PAM-sensitive and 11 L-PAM-resistant neuroblastoma cell lines. p53 was functional in seven/seven drug-sensitive but in only 4/11 drug-resistant cell lines ($P = 0.01$). In four of the seven cell lines lacking p53 function, mutations of p53 were detected by the microarray GeneChip p53 Assay and automated sequencing, whereas six cell lines with functional p53 had no evidence of p53 mutations. All of the cell lines with wild-type (wt) p53 showed a strong transactivation of the *p53-HBS/CAT* reporter gene, whereas the four cell lines with mutant p53 failed to transactivate p53 HBS/CAT. Overexpression of MDM2 protein (relative to p53 functional lines) was seen in two p53-nonfunctional cell lines with wt p53; one showed genomic amplification of MDM2. Nonfunctional and mutated p53 was detected in a resistant cell line, whereas a sensitive cell line derived from the same patient before treatment had functional and wt p53. Loss of p53 function was selectively achieved by transduction of human papillomavirus 16 E6 (which degrades p53) into two drug-sensitive neuroblastoma cell lines with intact p53, causing high-level drug resistance to L-PAM, carboplatin, and etoposide. These data obtained with neuroblastoma cell lines suggest that the high-level drug resistance observed in some recurrent neuroblastomas is attributable to p53 mutations and/or a loss of p53 function acquired during chemotherapy. If confirmed in patient tumor samples, these data support development of p53-independent therapies for consolidation and/or salvage of recurrent neuroblastomas.

INTRODUCTION

Neuroblastoma is a malignant childhood neoplasm of the sympathetic nervous system. Intensive chemoradiotherapy supported with autologous bone marrow transplantation has improved survival for high-risk neuroblastoma, especially if followed by 13-*cis*-retinoic acid (1). However, most high-risk neuroblastoma patients develop recurrent disease that is refractory to additional therapy (2). We have shown that during therapy neuroblastomas acquire a sustained high-level drug resistance, which correlates with the clinical therapy of the patient and the intensity of the therapy received (3).

p53 is a transcriptional regulatory protein (reviewed in Refs. 4 and 5), of which the target genes include: *p21*$^{WAF1/CIP1/SID1}$, *MDM2*, *Bax*, and *Gadd45*. Products of these genes are critical for cell cycle regulation, apoptosis, and DNA repair. In response to genotoxic stress, wt p53 exerts antiproliferative effects such as induction of cell cycle arrest and apoptosis. Inactivation of p53 results in genomic instability (6), and tumors either fail to arrest in G_1 or exhibit diminished apoptosis (7) and can be resistant to chemotherapeutic agents (8–10). p53 mutations and/or deletions have been linked to drug resistance in acute lymphoblastic leukemia (11); melanoma (12); osteosarcoma (13); and breast (14), ovarian (15), and testicular (16) cancers.

Mutations of p53 are commonly found in many human cancers (17) but are seen in only 2% of neuroblastoma tumors examined (18–23), with most p53 mutations observed in tumors coming from patients with progressive disease (18–20). As an alternative to mutations, cytoplasmic sequestration and defective translocation of p53 have been suggested as mechanisms of nonmutational inactivation (24), but several studies have shown that p53 function is intact in neuroblastoma cell lines (25–27).

Like neuroblastomas, mutations of p53 are infrequent in testicular cancers (28). However, a study of testicular cancers showed that for those tumors that either were resistant to initial chemotherapy or recurred with drug-resistant disease after therapy, p53 mutations were identified within exons 6–9 in 50% of tumor samples with teratomatous histology (16). On the basis of these observations we sought to determine whether drug resistance in neuroblastoma cell lines was associated with a lack of p53 function and/or p53 mutations.

We have examined p53 function by measuring p53 transcriptional activity in response to alkylating agent-mediated induction of p21 and MDM2 in a panel of neuroblastoma cell lines with a spectrum of resistance (acquired during therapy in patients) to L-PAM,[3] CBDCA, and ETOP, all commonly used drugs in neuroblastoma therapy. We examined the cell lines for p53 mutations by the GeneChip p53 Assay (29) and confirmed mutations by automated dideoxy DNA sequencing (29). In addition, we studied p53 function using a p53 transactivation assay (30). Finally, we abrogated p53 function by transducing drug-sensitive neuroblastoma cell lines with HPV16 E6, which targets cellular p53 for rapid degradation and renders cells expressing HPV16 E6 devoid of p53 function (31). We then determined sensitivities of HPV16 E6-transduced clones to L-PAM, CBDCA, and ETOP.

Here we show in a panel of neuroblastoma cell lines that a loss of p53 function is correlated with high-level drug resistance, that selective abrogation of p53 function can confer high-level drug resistance, and that loss of p53 function in neuroblastoma can be attributable to both mutational and nonmutational mechanisms.

MATERIALS AND METHODS

Cell Lines. We used a panel of 18 neuroblastoma cell lines (3, 32–34) obtained from patients at various points of disease: 3 at DX before any therapy (SK-N-BE(1), SMS-SAN, and CHLA-122), 2 at progressive disease during dual-agent induction therapy (SMS-LHN and SMS-KCNR), 6 at progressive

Received 2/15/01; accepted 6/8/01.

The costs of publication of this article were defrayed in part by the payment of page charges. This article must therefore be hereby marked *advertisement* in accordance with 18 U.S.C. Section 1734 solely to indicate this fact.

[1] Supported in part by the Neil Bogart Memorial Laboratories of the T. J. Martell Foundation for Leukemia, Cancer, and AIDS Research, and by National Cancer Institute Grants CA82830, CA60104, and CA31230.

[2] To whom requests for reprints should be addressed, at Division of Hematology-Oncology, MS# 57, Children's Hospital Los Angeles, 4650 Sunset Boulevard, Los Angeles, CA 90027. Phone: (323) 669-5646; Fax: (323) 664-9226 or 9455; E-mail: preynolds@chla.usc.edu.

[3] The abbreviations used are: L-PAM, melphalan; wt, wild-type; CBDCA, carboplatin; ETOP, etoposide; HPV, human papillomavirus; DX, diagnosis; FBS, fetal bovine serum; HBS, high-affinity binding site; CAT, chloramphenicol acetyl transferase; LC_{90}, drug concentration that was cytotoxic for 90% of the cell population; GSH, glutathione; HRP, horseradish peroxidase; ECL, enhanced chemiluminescence.

disease during intensive multiagent chemotherapy (SK-N-BE(2), SK-N-RA, LA-N-6, CHLA-119, CHLA-171, and CHLA-225), and 7 derived at relapse after bone marrow transplantation (CHLA-8, CHLA-51, CHLA-79, CHLA-90, CHLA-134, CHLA-136, and CHLA-172).

A neuroblastoma origin for CHLA-122, CHLA-119, and CHLA-172 cell lines was confirmed by reverse transcription-PCR detection of tyrosine hydroxylase (TH) RNA expression, which is a specific marker for neuroblastoma (3, 35). CHLA-225 showed no TH expression but did show a pattern for binding of the neuroblastoma-associated monoclonal antibody HSAN1.2 and the anti-HLA class I antibody W6–32 characteristic of neuroblastoma (3, 34). Other cell lines in the panel were described previously (3, 32–34).

SMS-SAN, SMS-LHN, and SK-N-RA were cultured in complete medium made from RPMI 1640 (Irvine Scientific, Santa Ana, CA) supplemented with 10% heat inactivated FBS (Gemini Bio-Products, Inc., Calabasas, CA). SMS-KCNR, SK-N-BE(1) SK-N-BE(2), LA-N-6, CHLA-122, CHLA-171, CHLA-225, CHLA-119, CHLA-51, CHLA-8, CHLA-79, CHLA-90, CHLA-134, CHLA-136, and CHLA-172 were cultured in complete medium made from Iscove's modified Dulbecco's medium (Bio Whittaker, Walkersville, MD) supplemented with ~3 mM L-glutamine (Gemini Bioproducts, Inc., Calabasas, CA), 5 μg/ml each of insulin and transferrin, 5 ng/ml of selenous acid (ITS Culture Supplement; Collaborative Biomedical Products, Bedford, MA), and 20% heat inactivated FBS. All of the cell lines used in the study were under passage 30, *Mycoplasma* free, and were cultured at 37°C in a humidified incubator containing 95% air + 5% CO_2 atmosphere without antibiotics. Because cell lines were not selected for resistance to drugs *in vitro*, drug-resistance represents selection that occurred in patients during therapy and correlates with those drugs used during therapy (3, 32).

Retroviral Infection. PA317 packaging cells transfected with the control retrovirus vector, pLXSN, or with the vector pLXSN16E6 (31) containing the HPV type 16 E6 gene, were obtained from American Type Culture Collection. Supernatant was harvested from the packaging cells and filtered through a 0.45-μM filter. SMS-SAN and SMS-LHN cells were then plated in retrovirus stock (three parts) with Polybrene (final concentration 0.5 μg/ml) and in complete medium composed of RPMI 1640 supplemented with 10% FBS (five parts). After a 5-h incubation, 5 ml of complete medium was added, and after overnight incubation cells were resuspended in fresh complete medium. Forty-eight h later cells were seeded into six-well plates in complete medium containing 250 μg/ml of G418. Individual clones were then picked and expanded in G418 containing medium. The integration of HPV16 E6 into G418-resistant clones was confirmed by Western blotting.

Drugs and Reagents. Antibodies p53 (DO-1) mouse monoclonal, p21 (C-19) rabbit polyclonal, MDM2 (SMP14) mouse monoclonal, and HRP-labeled secondary antimouse and antirabbit antibodies were purchased from Santa Cruz Biotechnology, Inc., Santa Cruz, CA. ECL Western blotting detection reagents were purchased from Amersham Pharmacia Biotech (Piscataway, NJ). ETOP was obtained from Bristol-Myers Squibb Co., Princeton, NJ; the NIH, Bethesda, MD provided L-PAM and CBDCA. Fluorescein diacetate was purchased from Eastman Kodak Company, Rochester, NY. Eosin Y and Polybrene (hexadimethrine bromide) were ordered from Sigma Chemical Co., St. Louis, MO.

Protein Expression. Proteins were extracted in radioimmunoprecipitation assay buffer (50 mM NaCl, 50 mM Tris, 1% Triton X-100, 1% sodium deoxycholate, and 0.1% SDS) and 40 μg (p53 and MDM2 expression) or 60 μg (p21 expression) of total protein was loaded per lane. Proteins were fractionated on 12–14% Tris-Glycine pre-cast gels (Novex, San Diego, CA), transferred to nitrocellulose membrane (Protran, Keene, NH), and probed with primary antibodies and then HRP-labeled secondary antibodies. Proteins were visualized using ECL Western blotting detection reagents.

GeneChip Probe Array. The GeneChip p53 Assay (Ref. 29; Affymetrix Inc., Santa Clara, CA) was used to detect mutated p53 sequences on exons 2–11 of 11 cell lines as described in the manufacturer's instructions. Briefly, 500 ng of genomic DNA, isolated using DNAzol Reagent (Life Technologies, Inc., Grand Island, NY), and the normal reference DNA were amplified with the PCR using the GeneChip p53 primer set and Taq DNA polymerase enzyme. The coding regions of the *p53* gene were amplified as 10 separate amplicons in a single reaction. Each PCR reaction contained genomic DNA, 5 μl of the p53 primer set (Affymetrix), 10 units of AmpliTaq Gold (Perkin-Elmer), PCR buffer II (Perkin-Elmer), 2.5 mM $MgCl_2$, and 0.2 mM each deoxynucleotide triphosphate in a final volume of 100 μl. PCR was carried out under the following conditions: heated at 95°C for 10 min; then 35 cycles of 95°C for 30 s, 60°C for 30 s, and 72°C for 45 s; followed by a final extension of 10 min at 72°C. Amplified cell line and reference DNA (45 μl) were fragmented with 0.25 units of fragmentation reagent (Affymetrix) at 25°C for 18 min in 2.5 units of calf intestine alkaline phosphatase, 0.4 mM EDTA, and 0.5 mM Tris-acetate (pH 8.2) followed by heat inactivation at 95°C for 10 min.

The DNA amplicons were labeled at 3′ ends with a fluoresceinated dideoxynucleotide using the terminal transferase enzyme. The fluorescently labeled DNA fragments were hybridized in a reaction containing 6 × saline-sodium phosphate-EDTA, 0.05% Triton X-100, 1 mg of acetylated BSA, and 2 nM control oligonucleotide F1 (Affymetrix) to the probes on the probe array for 30 min at 45°C, after which the probe array was washed [4 times with wash buffer (3 × SSPE, 0.005% Triton X-100)] and scanned with the GeneChip Scanner 50 with a laser that excites the fluorescent label. Thus, the amount of emitted light was proportional to DNA fragments on the probe array.

Data were analyzed using the GeneChip software. The software calculated the mean intensity of each probe cell. The hybridization intensities of the sample sequence were compared with those of a reference sequence, intensity patterns diverging from the reference were identified, and sites containing mutant bases were displayed. A score was assigned for each site containing a mutation or deletion. The higher the score for a given position, the greater the likelihood that site contained a mutant base. Scores exceeding 13 identified mutations (29).

Automated p53 Sequencing. Exons 5–8 of 11 neuroblastoma cell lines and exon 10 of one cell line were sequenced by the fluorescent dideoxy terminator method of cycle sequencing (29) on an ABI 377XL (96-well format) automated DNA sequencer at Laragen, Inc. (Los Angeles, CA). The primers were synthesized at Only DNA (Midland, TX) according to sequence information provided by Affymetrix GeneChip Assay in the manufacturer's booklet.

p53 Transactivation Assay. p53 status was also studied by transactivation assay (30). Cells were transiently transfected by calcium phosphate-DNA precipitation with a p53-HBS reporter plasmid containing two copies of a 20-bp motif encoding a p53-HBS ligated immediately upstream from a minimal thymidine kinase promoter linked to CAT. CAT expression occurs only when transcriptionally functional p53 binds to the HBS motif within the promoter. Cells were collected 48 h after transfection and assayed for CAT activity, determined the percentage conversion to the acetylated forms of [^{14}C]chloramphenicol measured by autoradiography of TLC. β-Galactosidase enzymatic activity (β-Galactosidase Enzyme Assay System with Reporter Lysis Buffer; Promega, Madison, WI) was used to standardize the efficiency of transfection.

Southern Blot Analysis. Aliquots of genomic DNA (20 μg) were digested with *Eco*RI, separated on 0.7% agarose gel and then transferred onto Hybond-N+ membranes (Amersham Pharmacia Biotech, Amersham, England). The blot was hybridized with a MDM2 cDNA probe labeled with [α-^{32}P]dCTP and filmed. MDM2 cDNA was cloned in the laboratory of Dr. B. Vogelstein (36). To confirm equal loading of DNA the blot was hybridized to β-actin (Clontech Laboratories, Inc., Palo Alto, CA). Human blood mononuclear cells were used as a reference for normal MDM2 copy number. Densitometric analysis of hybridization signals was performed using the Un-Scan-It Gel (Silk Scientific, Inc., Orem, Utah) software.

Cytotoxicity Assay. The cytotoxicity of L-PAM, ETOP, and CBDCA for neuroblastoma cell lines was determined using the DIMSCAN assay system, which has a 4 log dynamic range (3, 32, 34). The drug concentration ranges used were: L-PAM, 0–10 μg/ml; CBDCA, 0–5 μg/ml; and ETOP, 0–5 μg/ml. Each condition was tested in 12 replicates. Cells (1,000–15,000) were seeded in each well. After incubation of cell lines with L-PAM for 3 days, CBDCA for 7 days, and ETOP for 4 days, 10 μg/ml fluorescein diacetate was added to each well, plates were incubated for 30 min at 37°C, and finally 0.5% eosin Y was added. The total fluorescence was then measured using digital image microscopy, and results were expressed as surviving fractions of treated cells compared with control cells. LC_{90} values were calculated using the software "Dose-Effect Analysis with Microcomputers" (37). Cell lines with an L-PAM LC_{90} value >3.7 μg/ml [3.7 = 3 × the mean of LC_{90} values from the three cell lines (Table 1) established at DX before treatment] were considered drug resistant.

Statistical Analysis. Logarithmically transformed data of fractional cytotoxicity for SAN/E6, SAN/LXSN, LHN/E6, and LHN/LXSN clones were used

Table 1 *LC_{90} values of neuroblastoma and HPV 16E6 transfected clones of SMS-SAN and SMS-LHN cell lines*

	Phase of therapy	LC_{90} values (μg/ml)[a]			
		cell lines	L-PAM[b]	CBDCA[c]	ETOP[d]
Sensitive cell lines:	DX[e]	SK-N-BE(1)	0.8	0.2	0.2
	DX	SMS-SAN	1.3	0.7	0.1
	DX	CHLA-122	1.6	0.1	0.1
	PD-Ind_c[f]	SMS-LHN	2.1	1.3	2.1
	PD-Ind_c	SMS-KCNR	1.0	1.2	<0.1
	PD-BMT[g]	CHLA-8	0.3	2.3	<0.1
	PD-BMT	CHLA-51	2.2	2.6	<0.1
Resistant cell lines:	PD-Ind_i[h]	SK-N-BE(2)	24.0	2.1	1.1
	PD-Ind_i	SK-N-RA	37.5	>10.0	181.5
	PD-Ind_i	LA-N-6	15.4	8.6	27.3
	PD-Ind_i	CHLA-119	7.4	6.6	20.5
	PD-Ind_i	CHLA-171	68.9	11.6	443.6
	PD-Ind_i	CHLA-225	8.4	2.4	0.5
	PD-BMT	CHLA-79	5.0	3.2	12.6
	PD-BMT	CHLA-90	375.0	13.8	51.3
	PD-BMT	CHLA-134	37.1	26.3	256.0
	PD-BMT	CHLA-136	17.0	2.6	56.7
	PD-BMT	CHLA-172	101.4	43.4	31.2
Transduced clones:		SAN-LXSN[i]	1.8	1.3	0.7
		SAN/EG D4[j]	8.3	19.6	29.1
		SAN/E6 B3[j]	10.8	31.7	110.4
		LHN/LXSN[i]	4.7	6.4	3.7
		LHN/E6 2–6[j]	13.1	52.5	7.6
		LHN/E6 5-B5[j]	32.1	693.5	166.2

[a] Drug concentration that was cytotoxic for 90% of treated cells.
[b] Melphalan (Reference drug level for resistance defined as 3 × mean of LC_{90} values of cell lines established at diagnosis = 3.7 μg/ml).
[c] Carboplatin (Reference drug level for resistance = 1 μg/ml).
[d] Etoposide (Reference drug level for resistance = 0.4 μg/ml).
[e] Cell lines established from the patients before treatment.
[f] Cell lines established from patients at the time of disease progression after dual-agent induction chemotherapy.
[g] Cell lines established from patients at the time of disease progression after marrow ablative chemoradiotherapy followed by bone marrow transplantation.
[h] Cell lines established from patients at the time of disease progression after intensive multiagent chemotherapy.
[i] Empty vector controls of SMS-SAN and SMS-LHN cell lines.
[j] HPV 16 E6 clones of SMS-SAN and SMS-LHN cell lines.

for ANOVA analysis. SAN/E6 clones were compared with SAN/LXSN controls, and LHN/E6 clones were compared with LHN/LXSN controls. Linear contrasts were used to compare for difference in fractional cytotoxicity at each dose level between transfected clones. Statistical significance was designed as $P < 0.05$. To perform statistical analysis SAS software was used (SAS Institute, Inc., Cary, NC).

Fisher's exact test was performed to determine the correlation between drug resistance and p53 loss of function. Statistical significance was designed as $P < 0.05$.

RESULTS

Cell Line Panel. The cell lines used in this study and their drug sensitivity profile to L-PAM, CBDCA, and ETOP are shown in Table 1. The concentration of drug lethal for 90% of treated cells (LC_{90}) was calculated from dose-response curves for each drug tested using the DIMSCAN assay, which provides a 4 log dynamic range (3). Dose-response curves for three representative cell lines treated with L-PAM, CBDCA, and ETOP are shown in Fig. 1. Cell lines with an L-PAM LC_{90} value >3.7 μg/ml (3 × mean of cell lines established at DX before treatment) were considered resistant. We studied seven sensitive and 11 resistant cell lines. All 11 L-PAM-resistant cell lines showed cross-resistance to CBDCA (reference drug concentration = 1 μg/ml) and ETOP (reference drug concentration = 0.4 μg/ml).

Expression of p53, p21, and MDM2 in Neuroblastoma Cell Lines. Expression was measured by immunoblotting the basal expression and induction of p53, p21, and MDM2 (the latter two as indices of p53 function) 16 h after challenge by 6 μg/ml L-PAM, (Fig. 2*a*). Normally, wt p53 expression is either undetectable or very low but increases briefly on exposure to DNA-damaging agents. In contrast, stabilization of p53 in the absence of genotoxic stress is a hallmark of mutation and can be detected by immunoblotting (38). We found that p53 steady-state expression was low and inducible (≥2.5-fold), in seven/seven drug-sensitive cell lines: SK-N-BE(1), SMS-SAN, CHLA-122, SMS-LHN, SMS-KCNR, CHLA-8, and CHLA-51, and in 3/11 drug-resistant cell lines: LA-N-6, CHLA-79, and CHLA-136. A failure to induce p53 (≤2.5-fold) was observed in 8/11 drug-resistant cell lines: SK-N-BE(2), SK-N-RA, CHLA-119, CHLA-225, CHLA-171, CHLA-90, CHLA-134, and CHLA-172.

Cell lines that failed to induce p21 and/or MDM2 ≥1.5-fold (median p21 and MDM2 inductions) were defined as p53 nonfunctional. All seven drug-sensitive cell lines [SK-N-BE(1), SMS-SAN, CHLA-122, SMS-LHN, SMS-KCNR, CHLA-8, and CHLA-51] and 4/11 drug-resistant cell lines (LA-N-6, CHLA-79, CHLA-136, and SK-N-RA) demonstrated p21 and/or MDM2 induction after L-PAM challenge. Seven of the 11 drug-resistant-cell lines [SK-N-BE(2), CHLA-119, CHLA-171, CHLA-225, CHLA-90, CHLA-134, and CHLA-172] lacked functional p53 (Fig. 2, *b* and *c*). Thus, there was a significant correlation between drug resistance and p53 loss of function ($P = 0.01$).

Analysis of p53 Mutations. (Table 2). The Affymetrix GeneChip p53 Assay was used to analyze exons 2–11 for p53 mutations. Then, automated fluorescence dideoxynucleotide sequencing was used to confirm the Affymetrix GeneChip findings by analyzing exons 5–8 (where the most mutations were found). Sequencing of exon 10 was also carried out by automated sequencing for CHLA-119 to confirm a mutation detected by the GeneChip p53 Assay.

Wt p53 was found in six cell lines with functional p53 [SK-N-BE(1), SMS-LHN, LA-N-6, SK-N-RA, CHLA-79, and CHLA-136],

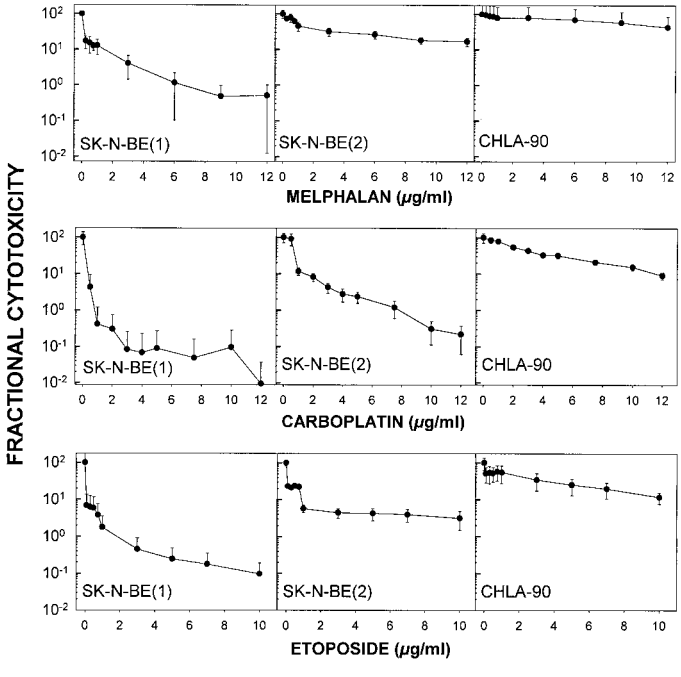

Fig. 1. Representative dose-response curves obtained by DIMSCAN assay. SK-N-BE(1) was established at DX before treatment. SK-N-BE(2) was established at the time of relapse after conventional induction chemotherapy and CHLA-90 at relapse after myeloablative chemoradiotherapy followed by bone marrow transplantation. Cell lines were treated with melphalan, carboplatin, and etoposide. Dose-response curves show the decreased drug sensitivity in cell lines established after induction chemotherapy and myeloablative chemoradiotherapy compared with cell lines established before treatment.

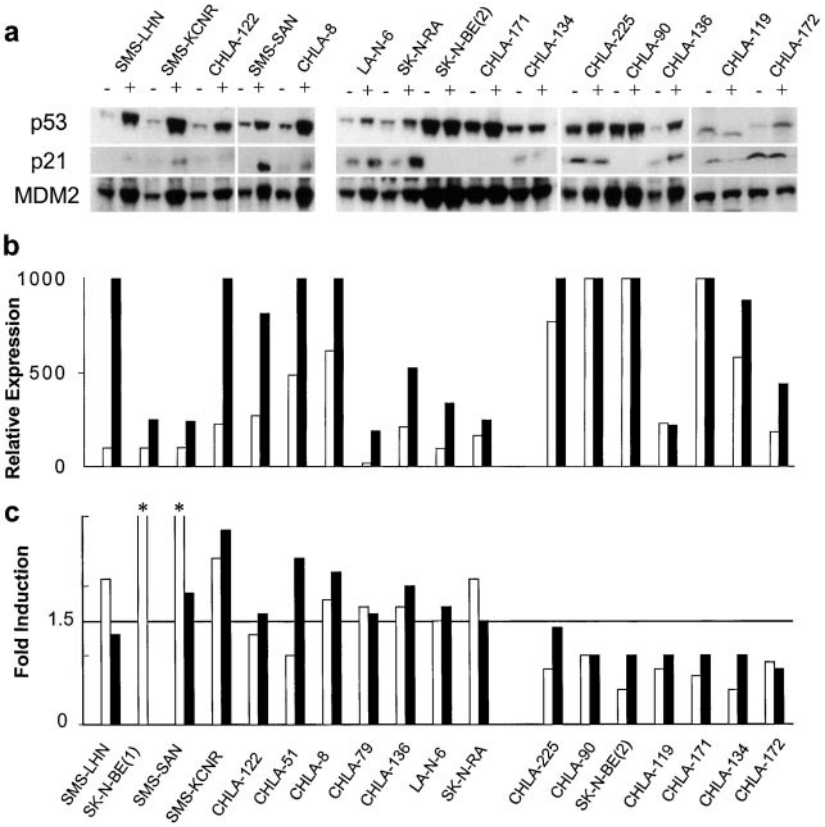

Fig. 2. *a*, Western blot analysis of p53, p21, and MDM2 expressions. −, protein steady state expressions; +, protein expression after 6 μg/ml L-PAM exposure for 16 h. *b*, quantitative analysis of p53 Western blots. Steady state (□) and induced levels (■) by 6 μg/ml L-PAM exposure (16 h) are shown. *c*, quantitative analysis for p21 (□) and MDM2 (■) induction by 6 μg/ml L-PAM (16 h) as assessed by Western blotting. *, off-scale values of SK-N-BE(1) and SMS-SAN for p21 induction were 23 and 40, respectively. *Horizontal line*, median induction value of 1.5 for p21 and MDM2, which was used as a cutoff for significant induction.

and in three of the seven cell lines with nonfunctional p53 (CHLA-225, CHLA-171, and CHLA-134). Mutations of p53 were found by both automated sequencing and the GeneChip Assay in four of the seven cell lines lacking functional p53 [SK-N-BE(2), CHLA-119, CHLA172, and CHLA-90].

p53 Transactivation Assay. (Fig. 3). We tested eight cell lines with functional p53 (SMS-LHN, CHLA-122, CHLA-51, CHLA-8, SK-N-RA, LA-N-6, CHLA-79, and CHLA-136) and all seven of the cell lines with nonfunctional p53 [CHLA-225, CHLA-134, CHLA-171, SK-N-BE(2), CHLA-90, CHLA-119, and CHLA-172] for their ability to transactivate a p53-HBS reporter gene construct. We could not carry out this assay for all of the cell lines because of an inability to transfect to some of the lines. CAT activity was detected (and, by inference, p53 transactivation) in all of the cell lines with wt p53, but in two cell lines (SMS-LHN and LA-N-6) CAT activity was lower than the other cell lines. The four cell lines with mutated p53 [SK-N-BE(2), CHLA-90, CHLA-119, and CHLA172] showed no transactivation of the p53-HBS reporter gene construct.

Table 2 *Sequence analysis of p53 in neuroblastoma cell lines*

Cell lines	Exon	Codon	Nucleotide change	Amino acid change	Induction of p21 and/or MDM2[a]	MDM2	
						Protein[b]	DNA[c]
Representative drug-sensitive cell lines							
SK-N-BE(1)			wt[d]		+	+	−
SMS-LHN			wt[d]		+	+	−
Drug-resistant cell lines							
LA-N-6			wt[e]		+	+	−
SK-N-RA			wt[e]		+	+	−
CHLA-79			wt[f]		+	+	−
CHLA-136			wt[e]		+	+	−
CHLA-171			wt[e]		−	↑ ↑	−
CHLA-225			wt[e]		−	↑	−
CHLA-134			wt[e]		−	↑	+
SK-N-BE(2)	5	135	TGC → TTC[e]	Cys → Phe	−	↑ ↑	nt
CHLA-119[g]	10	342	CGA → CTA[e]	Arg → Leu	−	↑	nt
CHLA-90	8	286	GAA → AAA[e]	Glu → Lys	−	↑ ↑	nt
CHLA-172	6	216	GTG → TTG[e]	Val → Leu	−	↑	nt

[a] Induction of p21 and/or MDM2 were used as indices of p53 function: +, induction of p21 and/or MDM2 by L-PAM challenge, −, failure to induce p21 or MDM2 by L-PAM challenge.

[b] Basal MDM2 protein expression by immunoblotting: +, protein is expressed; ↑, 1.1 to 1.4 times higher than median basal expression of MDM2; ↑ ↑, 1.7 to 2 times higher than median basal expression of MDM2.

[c] Genomic amplification of MDM2: +, amplified MDM2; −, nonamplified MDM2; nt, not tested.

[d] Studied using the GeneChip p53 Assay.

[e] Identical results were obtained by GeneChip p53 Assay and automated sequencing.

[f] Studied using the automated sequencing.

[g] In addition to the above mutation in CHLA-119, a polymorphism at codon 213 (a silent alteration of CGA to CGG) was also detected.

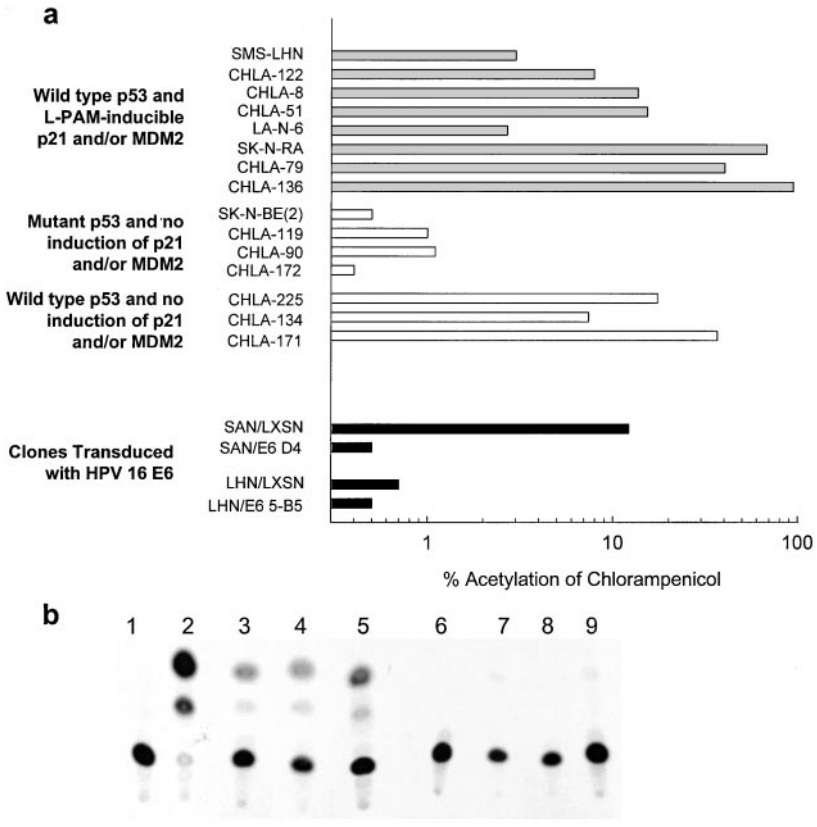

Fig. 3. p53 transactivation assay. *a*, *bars*, conversion values (%) of acetylated forms of chloramphenicol from total chloramphenicol. Cell lines with functional p53 (inducible p21 and/or MDM2) ▨, cell lines with nonfunctional p53 □, and transfected clones ■. *b*, results of CAT assay for three representative cell lines with functional p53 and four cell lines with mutated p53. SKOV-3 human ovarian carcinoma cell line (p53 null) was used as a negative control (*Lane 1*), and SKOV-3 cell line transfected with wt p53-HSP promoter was used as a positive control (*Lane 2*). *Lane 3*, CHLA-225; *Lane 4*, CHLA-134; *Lane 5*, CHLA171; *Lane 6*, SK-N-BE(2); *Lane 7*, CHLA-90; *Lane 8*, CHLA-172; and *Lane 9*, CHLA-119. CAT activation was visualized by TLC as acetylated form of ^{14}C-labeled chloramphenicol.

MDM2 Gene Amplification. A high baseline expression of MDM2 protein was seen in four of the seven cell lines lacking p53 function (Fig. 2) including two of the three p53 nonfunctional cell lines with wt p53 (CHLA-134 and CHLA-171). Genomic DNA from 11 cell lines and from normal human lymphocytes was analyzed for MDM2 amplification using Southern blot analysis. Genomic amplification of MDM2 was detected in only one cell line (CHLA-134), which showed a signal 6–14 × greater than the other samples analyzed (Fig. 4).

Paired Cell Lines. Within the panel studied, there were pairs of cell lines derived from two patients: one cell line at DX before treatment and then another after disease progression. SK-N-BE(1) was established at DX and then SK-N-BE(2) was established from the same patient at disease progression during nonmyeloablative (induction) chemotherapy. Similarly, CHLA-122 was established at DX and then from the same patient, CHLA-136 was established at time of relapse after myeloablative therapy supported with bone marrow transplantation. LC_{90} values of SK-N-BE(2) were 30 × greater for L-PAM, 13 × for CBDCA, and 7 × for ETOP relative to SK-N-BE(1); Table 1. SK-N-BE(1) had functional (Fig. 2, *b* and *c*) and wt p53 (Table 2), whereas SK-N-BE(2) showed a lack of functional p53 by p21/MDM2 induction (Fig. 2, *a–c*) and by p53 transactivation assay (Fig. 3), and showed mutation of p53 (Table 2). CHLA-136 showed drug resistance relative to CHLA-122, and LC_{90} values of CHLA-136 were 10.6 × greater for L-PAM, 26 × for CBDCA and 567 × for ETOP compared with CHLA-122 (Table 1). However, drug-resistance acquired by CHLA-136 was not associated with a loss of p53 function (Figs. 2 and 3) or p53 mutation (Table 2).

Selective Abrogation of p53 Function with HPV16 E6 Confers Multidrug Resistance. (Table 1; Fig. 5). To abrogate p53 activity in drug-sensitive, p53-functional neuroblastoma cell lines, we transduced the papillomavirus gene HPV16 E6 (which encodes a protein that promotes degradation of p53 and renders cells p53 nonfunctional; Ref. 31) into two drug-sensitive neuroblastoma cell lines. SMS-SAN (*MYCN* gene amplified) and SMS-LHN (*MYCN* nonamplified) were transduced with HPV16 E6 or with the pLXSN retrovirus empty vector as a control, and G418-resistant clones were selected from each. We then compared the sensitivity to L-PAM, CBDCA, and ETOP of HPV16 E6-transduced clones to the parental cell lines and pLXSN (empty vector) transduced controls. Reduced p53 activity was confirmed by the lack of p53 induction in L-PAM-challenged samples using Western blotting (data not shown) and the p53 transactivation assay (Fig. 3). Transduction of HPV16 E6 conferred high-level multidrug resistance to both SMS-SAN and SMS-LHN. LC_{90} values of SAN/E6 clones were 4.5–6 × higher for L-PAM, 15.4–25 × for CBDCA, and 41.6–157.7 × for ETOP relative to SAN/LXSN controls. Similarly, LC_{90} values of LHN/E6 clones were 3–7 × higher for L-PAM, 8–109 × for CBDCA, and 2–45.3 × for ETOP relative to LHN/LXSN cells.

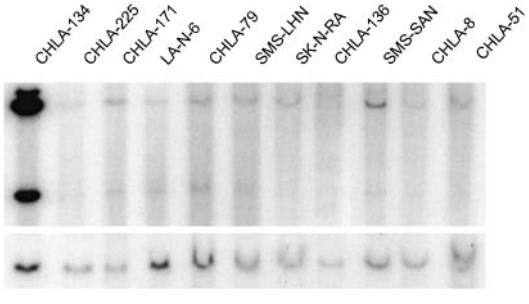

Fig. 4. Southern blot analysis of MDM2 gene amplification. *Eco*RI digested DNA samples were hybridized with an MDM2 cDNA probe (*top*) and as a control with β-actin probe (*bottom*).

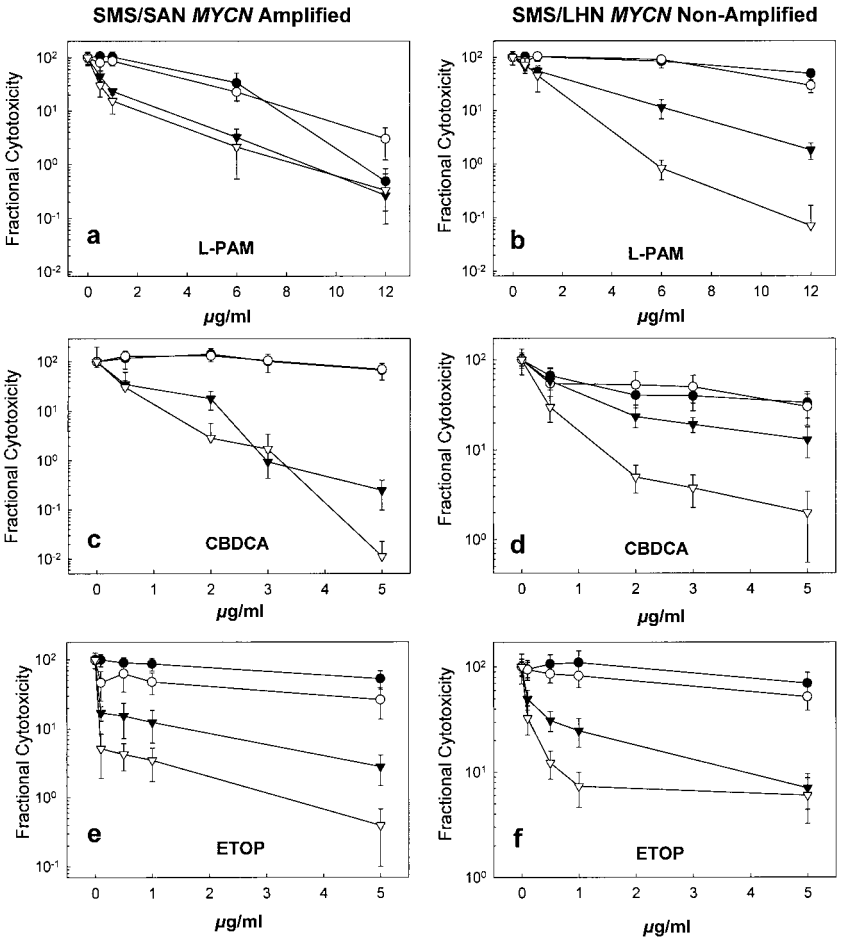

Fig. 5. Dose-response curves of neuroblastoma cell lines and their transfected clones. *a* and *b*, dose-response curves to L-PAM. *c* and *d*, dose-response curves to CBDCA. *e* and *f*, dose-response curves to ETOP. *a*, *c*, and *e*, cytotoxicity assays of SMS-SAN parental cell line (▽), SAN/E6 clones (○ and ●), and SAN/LXSN empty vector clone (▼) to L-PAM, CBDCA, and ETOP. *b*, *d*, and *f*, cytotoxicity assays of SMS-LHN parental cell line (▽), LHN/E6 clones (○ and ●), and LHN/LXSN empty vector clone (▼) to L-PAM, CBDCA, and ETOP. *P*s were calculated based on contrasts from ANOVA (see "Materials and Methods"). Generally, HPV16 E6 transfected clones were more resistant ($P \leq 0.002$) to all drugs than LXSN controls, and fractional cytotoxicity for the two transfected clones were not different ($P > 0.05$) for most drug concentrations.

DISCUSSION

Although most neuroblastomas show a good response to initial chemotherapy, tumors from many patients with high-risk disease (stage IV diagnosed after 1 year of age and/or tumor with *MYCN* amplification) acquire drug resistance during the therapy (1, 2). Neuroblastomas established as cell lines and maintained without drug exposure *in vitro* manifest drug resistance that was acquired in patients and correlates with the intensity of chemotherapy employed *in vivo*, suggesting that selection occurs for tumor cells resistant to those drugs used during therapy (3, 32). Identification of the molecular events conferring drug resistance in neuroblastoma may allow developing therapies to overcome the particular form of drug resistance manifested by this tumor and could provide markers to identify patients likely to develop progressive disease when treated with currently available chemotherapeutic agents.

As p53 mutations are infrequent in primary neuroblastomas (18–23), it has been suggested that functionally inactive p53 is attributable to cytoplasmic localization of p53 (24). Goldman *et al.* (25) reported that although p53 showed mainly cytoplasmic localization in neuroblastoma cell lines, p53 levels increased mainly in the nucleus after γ irradiation and showed that transcriptional activity of p53 was intact. Other studies have confirmed the presence of functional p53 in neuroblastoma cell lines in response to γ irradiation (39), UV light (26), and cisplatin (27).

It is well known that p53 mediates responses to cytotoxic agents (8, 40) and that mutant p53 is correlated with resistance to DNA-damaging agents (11, 14, 16, 41). Here we have shown that for 18 neuroblastoma cell lines, p53 loss of function correlated with drug resistance ($P = 0.01$). Using Western blot analysis for p53 target genes, we found that p53 was functional, as determined by transcriptionally intact p53 (induction of p21 and/or MDM2 after 16 h of 6 μg/ml L-PAM) in seven/seven drug-sensitive cell lines. Moreover, the low steady-state expression and inducible p53 observed in these cell lines also suggested the presence of functional p53.

We found that p53 was nonfunctional in 7 of 11 drug-resistant cell lines [SK-N-BE(2), CHLA-119, CHLA-225, CHLA-171, CHLA-90, CHLA-134, and CHLA-172] as demonstrated by a failure to induce downstream genes (p21 and MDM2) by L-PAM. High steady state p53 expression, a hallmark of p53 mutation (38), was found only in cell lines with nonfunctional p53 [SK-N-BE(2), CHLA-225, CHLA-171, CHLA-90, and CHLA-134].

Sequence analysis for p53 of all seven cell lines with loss of p53 function was performed by both the Affymetrix GeneChip p53 Assay and automated sequencing using the fluorescent dideoxy terminator method. First, we analyzed exons 2–11 by the GeneChip p53 Assay and then exons 5–8 (DNA-binding region) using automated DNA sequencing. As the Affymetrix GeneChip Assay provides far greater sensitivity for detection of p53 mutations than does automated DNA sequencing (29), we sequenced only exons 5–8 (where most of mutations were located) by automated sequencing to confirm the findings of the Affymetrix GeneChip Assay; to confirm a mutation identified by the GeneChip Assay, exon 10 was also sequenced in CHLA-119. We found mutations in the DNA-binding domain in SK-N-BE(2), CHLA-90, and CHLA-172 (CHLA-119 harbors a polymorphism in this region), all of which were drug-resistant cell lines with nonfunctional p53 that were derived from heavily treated pa-

tients. These mutations have been identified previously in various tumors.[4] In addition to mutations in the DNA binding region, we identified a mutation in exon 10 in CHLA-119, which can also render p53 nonfunctional (42). Mutations of p53 were not found in CHLA-225, CHLA-171, and CHLA-134 using either the GeneChip p53 Assay or automated p53 sequencing. As expected, two representative drug-sensitive/p53-functional cell lines [SK-N-BE(1) and SMS-LHN] showed no p53 mutations by the GeneChip p53 Assay.

Only 4/11 drug-resistant cell lines (LA-N-6, SK-N-RA, CHLA-79, and CHLA-136) had functional p53 (as demonstrated by induction of p21 and/or MDM2 in response to L-PAM), and all 4 cell lines had wt p53 by both automated p53 sequencing and GeneChip p53 Assay. It is possible that genetic alterations in apoptotic events downstream of p53, *e.g.*, Bax (7) or caspase-8 (43), could account for drug resistance seen in these cell lines. Data from tumors other than neuroblastoma have shown that decreased L-PAM uptake (44) or increased GSH biosynthesis (45), together with increased export of GSH-alkylator complex (46), are also associated with drug resistance. One or more of these may account for the drug resistance observed in neuroblastoma cell lines with intact p53 function. However, our data suggest that the most frequent event conferring high-level, multidrug resistance in neuroblastomas is a loss of p53 function.

MDM2 is a transcriptional target of p53, which regulates p53 expression in a negative regulatory feedback fashion. The role of MDM2 has been implicated in the pathogenesis of cancer via inhibition of p53 tumor suppressor function, and MDM2 overexpression attributable to *MDM2* gene amplification or increased translation can inactivate p53 (47, 48). There were three cell lines (CHLA-225, CHLA-171, and CHLA-134) in our panel that displayed increased accumulation and stabilization of p53 and failed to induce p21 and MDM2 proteins after L-PAM challenge (Fig. 2). All three had wt p53, and unlike the cells with mutant p53, these three cell lines showed intact p53 transactivation using the *p53-HBS/CAT* reporter gene (Fig. 3). Two of these cell lines (CHLA-171 and CHLA-134) showed overexpression of MDM2 protein by Western blotting, and we found genomic amplification of MDM2 in one of these cell lines (CHLA-134) by Southern blotting. Thus, MDM2 protein overexpression is likely one mechanism by which p53 function is compromised in some neuroblastomas.

The level of expression of unstimulated MDM2 protein was high in two neuroblastoma cell lines with mutated p53 [SK-N-BE(2) and CHLA-90; Fig. 2]. It has been shown that MDM2 can be stabilized by mutant p53 and proposed that it occurs because of inhibition of MDM2 ubiquitination after forming a complex with mutant p53 (49).

To demonstrate that a loss of p53 function mediates multidrug resistance in neuroblastoma we transduced two sensitive neuroblastoma cell lines carrying functional p53 with the HPV type 16 gene (HPV16 E6). HPV16 E6 protein and cellular E6-associated protein form a complex and function as a ubiquitin ligase for p53 for increased degradation, thus disrupting the p53-mediated response (31). HPV16 E6-transformed cells have been used to examine the effect of p53 loss on genomic stability, apoptosis, and sensitivity to chemotherapeutic agents or ionizing radiation (50–52). As *MYCN* amplification has been linked to tumor progression and poor outcome in neuroblastomas (53), we used *MYCN* amplified (SMS-SAN) and *MYCN* nonamplified (SMS-LHN) cell lines for these experiments. The LC_{90} values of two separate HPV16 E6 clones of both cell lines were increased relative to the pLXSN empty vector controls: 3–7 times for L-PAM; 8–109 times for CBDCA; and 2–158 times for ETOP. Decreased sensitivity of pLXSN empty vector clones compared with parental cells was observed in both cell lines, suggesting that selection for resistance to G418 can mediate modest cross resistance to chemotherapeutic drugs.

We showed that p53 is functional in all of the tested neuroblastoma cell lines established before chemotherapy [SK-N-BE(1), SMS-SAN, and CHLA-122] and that loss of p53 function appears to be one of the major mechanisms responsible for high-level multidrug resistance in neuroblastoma. In one pair of cell lines derived from the same patient before treatment [SK-N-BE(1)] and then after disease progression on induction chemotherapy [SK-N-BE(2)], we demonstrated acquisition of a drug-resistant phenotype (3, 32), which we and others (54–56) showed was associated with acquisition of a p53 mutation on codon 135 and the loss of p53 function. This is consistent with previous observations that neuroblastomas lacking p53 mutations at DX showed mutations of p53 in tumors obtained at relapse after chemotherapy (19, 20). These observations, combined with the high frequency of p53 mutations and loss of p53 function in chemotherapy-resistant cell lines relative to those established at DX, suggests that selection for neuroblastoma cells with p53 mutations and/or loss of p53 function (in some cases attributable to overexpression of MDM2) occurs during therapy, leading to multidrug resistance. As all of the drug-sensitive neuroblastoma cell lines had functional p53 and lacked p53 mutations, it is unlikely that loss of p53 function was acquired as a result of growth *in vitro*.

Our data suggest that the relationship of p53 mutations and/or functionality to drug resistance should be investigated in tumor samples from patients with neuroblastoma. One possible approach to studying clinical samples is the Affymetrix GeneChip p53 Assay. The GeneChip p53 Assay (recently developed by Affymetrix Inc.) is an oligonucleotide microarray approach that provides an accurate, sensitive, and specific method for detection of p53 mutations (29, 57, 58). Our results confirm that the GeneChip Assay reliably detects p53 mutations. However, as loss of p53 function in some cell lines occurred without p53 mutations, methods for detecting p53 functionality in clinical specimens may also be required to complement detection of mutations. We are currently analyzing p53 mutations in tumor samples obtained from patients in which the tumor persisted or progressed after chemotherapy. Confirmation with patient tumors that inactivation of p53 correlates with a poor response to chemotherapy in neuroblastoma would additionally support a focus on p53-independent therapies (*e.g.*, ceramide modulators; Refs. 27, 59), L-PAM in combination with the GSH depletor buthionine sulfoximine (34, 60), immunotherapy (61), or antimicrotubule agents (62, 63) for neuroblastomas recurring after chemotherapy.

[4] See the p53 website: http://perso.curie.fr/Thierry.Soussi/.

ACKNOWLEDGMENTS

We thank Dr. June Biedler for providing the SK-N-BE(1) and SK-N-BE(2) cell lines, Dr. Susan Groshen and Denice Wei for their help in statistical analysis, and Dr. Carl Miller for providing the MDM2 probe.

REFERENCES

1. Matthay, K. K., Villablanca, J. G., Seeger, R. C., Stram, D. O., Harris, R. E., Ramsay, N. K., Swift, P., Shimada, H., Black, C. T., Brodeur, G. M., Gerbing, R. B., and Reynolds, C. P. Treatment of high-risk neuroblastoma with intensive chemotherapy, radiotherapy, autologous bone marrow transplantation, and 13-*cis*-retinoic acid. Children's Cancer Group. N. Engl. J. Med., *341:* 1165–1173, 1999.
2. Seeger, R. C., and Reynolds, C. P. Treatment of high-risk solid tumors of childhood with intensive therapy and autologous bone marrow transplantation. Pediatr. Clin. N. Am., *38:* 393–424, 1991.
3. Keshelava, N., Seeger, R. C., Groshen, S., and Reynolds, C. P. Drug resistance patterns of human neuroblastoma cell lines derived from patients at different phases of therapy. Cancer Res., *58:* 5396–5405, 1998.

4. Ko, L. J., and Prives, C. p53: puzzle and paradigm. Genes Dev., *10:* 1054–1072, 1996.
5. May, P., and May, E. Twenty years of p53 research: structural and functional aspects of the p53 protein (published erratum appears in Oncogene, *19:* 1734, 2000). Oncogene, *18:* 7621–7636, 1999.
6. Malkin, D. p53 and the Li-Fraumeni syndrome. Biochim. Biophys. Acta, *1198:* 197–213, 1994.
7. McCurrach, M. E., Connor, T. M., Knudson, C. M., Korsmeyer, S. J., and Lowe, S. W. bax-deficiency promotes drug resistance and oncogenic transformation by attenuating p53-dependent apoptosis. Proc. Natl. Acad. Sci. USA, *94:* 2345–2349, 1997.
8. Lowe, S. W., Bodis, S., McClatchey, A., Remington, L., Ruley, H. E., Fisher, D. E., Housman, D. E., and Jacks, T. p53 status and the efficacy of cancer therapy *in vivo*. Science (Wash. DC), *266:* 807–810, 1994.
9. Perego, P., Giarola, M., Righetti, S. C., Supino, R., Caserini, C., Delia, D., Pierotti, M. A., Miyashita, T., Reed, J. C., and Zunino, F. Association between cisplatin resistance and mutation of *p53* gene and reduced bax expression in ovarian carcinoma cell systems. Cancer Res., *56:* 556–562, 1996.
10. Piovesan, B., Pennell, N., and Berinstein, N. L. Human lymphoblastoid cell lines expressing mutant p53 exhibit decreased sensitivity to cisplatin-induced cytotoxicity. Oncogene, *17:* 2339–2350, 1998.
11. Lam, V., McPherson, J. P., Salmena, L., Lees, J., Chu, W., Sexsmith, E., Hedley, D. W., Freedman, M. H., Reed, J. C., Malkin, D., and Goldenberg, G. J. *p53* gene status and chemosensitivity of childhood acute lymphoblastic leukemia cells to Adriamycin. Leuk. Res., *23:* 871–880, 1999.
12. Li, G., Tang, L., Zhou, X., Tron, V., and Ho, V. Chemotherapy-induced apoptosis in melanoma cells is p53 dependent. Melanoma Res., *8:* 17–23, 1998.
13. Asada, N., Tsuchiya, H., and Tomita, K. *De novo* deletions of *p53* gene and wild-type p53 correlate with acquired cisplatin-resistance in human osteosarcoma OST cell line. Anticancer Res., *19:* 5131–5137, 1999.
14. Berns, E. M., Foekens, J. A., Vossen, R., Look, M. P., Devilee, P., Henzen-Logmans, S. C., van Staveren, I. L., van Putten, W. L., Inganas, M., Meijer-van Gelder, M. E., Cornelisse, C., Claassen, C. J., Portengen, H., Bakker, B., and Klijn, J. G. Complete sequencing of TP53 predicts poor response to systemic therapy of advanced breast cancer. Cancer Res., *60:* 2155–2162, 2000.
15. Righetti, S. C., Perego, P., Corna, E., Pierotti, M. A., and Zunino, F. Emergence of p53 mutant cisplatin-resistant ovarian carcinoma cells following drug exposure: spontaneously mutant selection. Cell Growth Differ., *10:* 473–478, 1999.
16. Houldsworth, J., Xiao, H., Murty, V. V., Chen, W., Ray, B., Reuter, V. E., Bosl, G. J., and Chaganti, R. S. Human male germ cell tumor resistance to cisplatin is linked to *TP53* gene mutation. Oncogene, *16:* 2345–2349, 1998.
17. Harris, C. C. The Walter Hubert lecture–molecular epidemiology of human cancer: insights from the mutational analysis of the *p53* tumour-suppressor gene. Br. J. Cancer, *73:* 261–269, 1996.
18. Hosoi, G., Hara, J., Okamura, T., Osugi, Y., Ishihara, S., Fukuzawa, M., Okada, A., Okada, S., and Tawa, A. Low frequency of the *p53* gene mutations in neuroblastoma. Cancer (Phila.), *73:* 3087–3093, 1994.
19. Imamura, J., Bartram, C. R., Berthold, F., Harms, D., Nakamura, H., and Koeffler, H. P. Mutation of the *p53* gene in neuroblastoma and its relationship with *N*-myc amplification. Cancer Res., *53:* 4053–4058, 1993.
20. Manhani, R., Cristofani, L. M., Odone, F. V, and Bendit, I. Concomitant p53 mutation and MYCN amplification in neuroblastoma. Med. Pediatr. Oncol., *29:* 206–207, 1997.
21. Vogan, K., Bernstein, M., Leclerc, J. M., Brisson, L., Brossard, J., Brodeur, G. M., Pelletier, J., and Gros, P. Absence of *p53* gene mutations in primary neuroblastomas. Cancer Res., *53:* 5269–5273, 1993.
22. Castresana, J. S., Bello, M. J., Rey, J. A., Nebreda, P., Queizan, A., Garcia-Miguel, P., and Pestana, A. No TP53 mutations in neuroblastomas detected by PCR-SSCP analysis. Genes Chromosomes Cancer, *10:* 136–138, 1994.
23. Komuro, H., Hayashi, Y., Kawamura, M., Hayashi, K., Kaneko, Y., Kamoshita, S., Hanada, R., Yamamoto, K., Hongo, T., and Yamada, M. Mutations of the *p53* gene are involved in Ewing's sarcomas but not in neuroblastomas. Cancer Res., *53:* 5284–5288, 1993.
24. Ostermeyer, A. G., Runko, E., Winkfield, B., Ahn, B., and Moll, U. M. Cytoplasmically sequestered wild-type p53 protein in neuroblastoma is relocated to the nucleus by a C-terminal peptide. Proc. Natl. Acad. Sci. USA, *93:* 15190–15194, 1996.
25. Goldman, S. C., Chen, C. Y., Lansing, T. J., Gilmer, T. M., and Kastan, M. B. The p53 signal transduction pathway is intact in human neuroblastoma despite cytoplasmic localization. Am. J. Pathol., *148:* 1381–1385, 1996.
26. McKenzie, P. P., Guichard, S. M., Middlemas, D. S., Ashmun, R. A., Danks, M. K., and Harris, L. C. Wild-type p53 can induce p21 and apoptosis in neuroblastoma cells but the DNA damage-induced G1 checkpoint function is attenuated. Clin. Cancer Res., *5:* 4199–4207, 1999.
27. Maurer, B. J., Metelitsa, L. S., Seeger, R. C., Cabot, M. C., and Reynolds, C. P. Increase of ceramide and induction of mixed apoptosis/necrosis by *N*-(4-hydroxyphenyl)-retinamide in neuroblastoma cell lines. J. Natl. Cancer Inst., *91:* 1138–1146, 1999.
28. Heimdal, K., Lothe, R. A., Lystad, S., Holm, R., Fossa, S. D., and Borresen, A. L. No germline TP53 mutations detected in familial and bilateral testicular cancer. Genes Chromosomes Cancer, *6:* 92–97, 1993.
29. Ahrendt, S. A., Halachmi, S., Chow, J. T., Wu, L., Halachmi, N., Yang, S. C., Wehage, S., Jen, J., and Sidransky, D. Rapid p53 sequence analysis in primary lung cancer using an oligonucleotide probe array. Proc. Natl. Acad. Sci. USA, *96:* 7382–7387, 1999.
30. Chumakov, A. M., Miller, C. W., Chen, D. L., and Koeffler, H. P. Analysis of p53 transactivation through high-affinity binding sites. Oncogene, *8:* 3005–3011, 1993.
31. Scheffner, M., Huibregtse, J. M., Vierstra, R. D., and Howley, P. M. The HPV-16 E6 and E6-AP complex functions as a ubiquitin-protein ligase in the ubiquitination of p53. Cell, *75:* 495–505, 1993.
32. Keshelava, N., Groshen, S., and Reynolds, C. P. Cross-resistance of topoisomerase I and II inhibitors in neuroblastoma cell lines. Cancer Chemother. Pharmacol., *45:* 1–8, 2000.
33. Reynolds, C. P., Tomayko, M. M., Donner, L., Helson, L., Seeger, R. C., Triche, T. J., and Brodeur, G. M. Biological classification of cell lines derived from human extra-cranial neural tumors. Prog. Clin. Biol. Res., *271:* 291–306, 1988.
34. Anderson, C. P., Seeger, R. C., Satake, N., Meek, W. E., Keshelava, N., Bailey, H. H., Monforte-Munoz, H. L., and Reynolds, C. P. Buthionine sulfoximine and myeloablative concentrations of melphalan overcome resistance in melphalan-resistant neuroblastoma cell line. J. Pediatr. Hematol. Oncol., in press, 2001.
35. Wang, Y., Einhorn, P., Triche, T. J., Seeger, R. C., and Reynolds, C. P. Expression of protein gene product 9.5 and tyrosine hydroxylase in childhood small round cell tumors. Clin. Cancer Res., *6:* 551–558, 2000.
36. Oliner, J. D., Kinzler, K. W., Meltzer, P. S., George, D. L., and Vogelstein, B. Amplification of a gene encoding a p53-associated protein in human sarcomas. Nature (Lond.), *358:* 80–83, 1992.
37. Chou, J., and Chou, T. C. Multiple drug-effect analysis (program B). *In:* J. Chou and T. C. Chou (eds.), Dose-effect Analysis with Microcomputers, pp. 19–64. New York: Memorial Sloan-Kettering Cancer Center, 1987.
38. Blagosklonny, M. V. Loss of function and p53 protein stabilization. Oncogene, *15:* 1889–1893, 1997.
39. Jasty, R., Lu, J., Irwin, T., Suchard, S., Clarke, M. F., and Castle, V. P. Role of p53 in the regulation of irradiation-induced apoptosis in neuroblastoma cells. Mol. Genet. Metab., *65:* 155–164, 1998.
40. Lowe, S. W., Ruley, H. E., Jacks, T., and Housman, D. E. p53-dependent apoptosis modulates the cytotoxicity of anticancer agents. Cell, *74:* 957–967, 1993.
41. Lee, J. M., and Bernstein, A. p53 mutations increase resistance to ionizing radiation. Proc. Natl. Acad. Sci. USA, *90:* 5742–5746, 1993.
42. Rollenhagen, C., and Chene, P. Characterization of p53 mutants identified in human tumors with a missense mutation in the tetramerization domain. Int. J. Cancer, *78:* 372–376, 1998.
43. Teitz, T., Wei, T., Valentine, M. B., Vanin, E. F., Grenet, J., Valentine, V. A., Behm, F. G., Look, A. T., Lahti, J. M., and Kidd, V. J. Caspase 8 is deleted or silenced preferentially in childhood neuroblastomas with amplification of MYCN. Nat. Med., *6:* 529–535, 2000.
44. Pu, Q., Bianchi, P., and Bezwoda, W. R. Alkylator resistance in human B lymphoid cell lines: (1). Melphalan accumulation, cytotoxicity, interstrand-DNA-crosslinks, cell cycle analysis, and glutathione content in the melphalan-sensitive B-lymphocytic cell line (WIL2) and in the melphalan-resistant B-CLL cell line (WSU-CLL). Anticancer Res., *20:* 2561–2568, 2000.
45. Calvert, P., Yao, K. S., Hamilton, T. C., and O'Dwyer, P. J. Clinical studies of reversal of drug resistance based on glutathione. Chem.-Biol. Interact., *111–112:* 213–224, 1998.
46. Ishikawa, T., Bao, J. J., Yamane, Y., Akimaru, K., Frindrich, K., Wright, C. D., and Kuo, M. T. Coordinated induction of MRP/GS-X pump and γ-glutamylcysteine synthetase by heavy metals in human leukemia cells. J. Biol. Chem., *271:* 14981–14988, 1996.
47. Capoulade, C., Bressac-de Paillerets, B., Lefrere, I., Ronsin, M., Feunteun, J., Tursz, T., and Wiels, J. Overexpression of MDM2, due to enhanced translation, results in inactivation of wild-type p53 in Burkitt's lymphoma cells. Oncogene, *16:* 1603–1610, 1998.
48. Keleti, J., Quezado, M. M., Abaza, M. M., Raffeld, M., and Tsokos, M. The MDM2 oncoprotein is overexpressed in rhabdomyosarcoma cell lines and stabilizes wild-type p53 protein. Am. J. Pathol., *149:* 143–151, 1996.
49. Peng, Y., Chen, L., Li, C., Lu, W., Agrawal, S., and Chen, J. Stabilization of the MDM2 oncoprotein by mutant p53. J. Biol. Chem., *276:* 6874–6878, 2001.
50. Havre, P. A., Yuan, J., Hedrick, L., Cho, K. R., and Glazer, P. M. p53 inactivation by HPV16 E6 results in increased mutagenesis in human cells. Cancer Res., *55:* 4420–4424, 1995.
51. Tsang, N. M., Nagasawa, H., Li, C., and Little, J. B. Abrogation of p53 function by transfection of *HPV16 E6* gene enhances the resistance of human diploid fibroblasts to ionizing radiation. Oncogene, *10:* 2403–2408, 1995.
52. Meyn, M. S., Strasfeld, L., and Allen, C. Testing the role of p53 in the expression of genetic instability and apoptosis in ataxia-telangiectasia. Int. J. Radiat. Biol., *66:* S141–S149, 1994.
53. Seeger, R. C., Brodeur, G. M., Sather, H., Dalton, A., Siegel, S. E., Wong, K. Y., and Hammond, D. Association of multiple copies of the *N-myc* oncogene with rapid progression of neuroblastomas. N. Engl. J. Med., *313:* 1111–1116, 1985.
54. Kaghad, M., Bonnet, H., Yang, A., Creancier, L., Biscan, J. C., Valent, A., Minty, A., Chalon, P., Lelias, J. M., Dumont, X., Ferrara, P., McKeon, F., and Caput, D. Monoallelically expressed gene related to p53 at 1p36, a region frequently deleted in neuroblastoma and other human cancers. Cell, *90:* 809–819, 1997.
55. Keshelava, N., Zuo, J. J., Waidyaratne, N. S., Triche, T. J., and Reynolds, C. P. p53 mutations and loss of p53 function confer multidrug resistance in neuroblastoma. Med. Pediatr. Oncol., *35:* 563–568, 2000.
56. Tweddle, D., Malcolm, A., Bown, N., Pearson, A., and Lunec, J. Evidence for the development of p53 mutations after cytotoxic therapy in a neuroblastoma cell line. Cancer Res., *61:* 8–13, 2001.
57. Wen, W. H., Bernstein, L., Lescallett, J., Beazer-Barclay, Y., Sullivan-Halley, J., White, M., and Press, M. F. Comparison of TP53 mutations identified by oligonu-

cleotide microarray and conventional DNA sequence analysis. Cancer Res., *60:* 2716–2722, 2000.

58. Ahrendt, S. A., Decker, P. A., Doffek, K., Wang, B., Xu, L., Demeure, M. J., Jen, J., and Sidransky, D. Microsatellite instability at selected tetranucleotide repeats is associated with p53 mutations in non-small cell lung cancer. Cancer Res., *60:* 2488–2491, 2000.
59. Maurer, B. J., Melton, L., Billups, C., Cabot, M. C., and Reynolds, C. P. Synergistic cytotoxicity in solid tumor cell lines between *N*-(4-Hydroxyphenyl)retinamide and modulators of ceramide metabolism. J. Natl. Cancer Inst., *92:* 1897–1909, 2000.
60. Anderson, C. P., Keshelava, N., Satake, N., Meek, W. H., and Reynolds, C. P. Synergism of buthionine sulfoximine and melphalan against neuroblastoma cell lines derived after disease progression. Med. Pediatr. Oncol., *35:* 659–662, 2000.
61. Cheung, N. V., and Yu, A. L. Immunotherapy of neuroblastoma. *In:* G. M. Brodeur, T. Sawada, Y. Tsuchida, and P. A.Voute (eds.), Neuroblastoma, pp. 1541–1546. Amsterdam: Elsevier Science, 2000.
62. Lavarino, C., Pilotti, S., Oggionni, M., Gatti, L., Perego, P., Bresciani, G., Pierotti, M. A., Scambia, G., Ferrandina, G., Fagotti, A., Mangioni, C., Lucchini, V., Vecchione, F., Bolis, G., Scarfone, G., and Zunino, F. *p53* gene status, and response to platinum/paclitaxel-based chemotherapy in advanced ovarian carcinoma. J. Clin. Oncol., *18:* 3936–3945, 2000.
63. King, T. C., Akerley, W., Fan, A. C., Moore, T., Mangray, S., Hsiu, C. M., and Safran, H. p53 mutations do not predict response to paclitaxel in metastatic nonsmall cell lung carcinoma. Cancer (Phila.), *89:* 769–773, 2000.